

Materno-Fetal and Teratogenic Effects of Different Size Gold Nanoparticles (AuNPs) in Pregnant Rats

Ahmed Sabry Abdoon^{1*}; Othman F Abdelzaher²; Eman S Mahmoud³; Ahmed BM Mehany²; Fathy E Mohammed²; Mohamed I Rady²

¹Department of Animal Reproduction, Veterinary Research Division, National Research Centre, Dokki 12622, Cairo, Egypt.

²Department of Histology, Faculty of Science, Al-Azhar University, Egypt.

³Departments of Histology and Physiology Faculty of Medicine for Girls (Cairo), Al-Azhar University, Egypt.

Corresponding Author: Ahmed S Abdoon

Department of Animal Reproduction and Artificial Insemination, Veterinary Research Division, National Research Centre (NRC), Tahrir St., Dokki 12622, Cairo, Egypt.

Tel: +201001662430; +20122194122; +20233370931;

Email: assabdoon@yahoo.com

Article information

Received: Sep 19, 2023

Accepted: Oct 24, 2023

Published: Oct 31, 2023

SciBase Oncology - scibasejournals.org

Sabry Abdoon A et al. © All rights are reserved

Citation: Abdoon AS, Abdelzaher OF, Mahmoud ES, Mehany ABM, Mohammed FE, et al. Materno-Fetal and Teratogenic Effects of Different Size Gold Nanoparticles (Aunps) in Pregnant Rats. SciBase Oncol. 2023; 1(2): 1006.

Abstract

The widespread use of gold nanoparticles (AuNPs) in many fields has increased; however, their potential effects on embryo-fetal development have not been explored. This study was designed to investigate the potential effects of different sizes of gold nanoparticles (AuNPs) on maternal and embryo-fetal development in rats. Forty-eight early pregnant Albino rats (48 h after mating) were divided into: The first group served as a control, for the 2nd, 3rd and 4th groups, pregnant rats were Intraperitoneally (i.p.) injected with 75 µg of 10 nm, 25 nm or 50 nm AuNPs/kg body weight. Control and experimental dams were scarified on Days-10, 15 and 19 of gestation. Uteri were dissected out to evaluate the intrauterine pregnancy rate, fetal resorption, histopathological changes in uterine and placental tissues, and localization of AuNPs in placenta using TEM, fetal weight and skeletal malformation in fetus. Results indicated that early pregnant rats treated with 10 nm AuNPs showed a symmetrical distribution of fetuses in uterine horns, decrease in implantation rate, decreased fetal weight and induced severe skeletal anomalies on Day-19 of gestation. Also, all AuNPs induced sever histopathological changes in uterine wall and placenta. Ten nanometer AuNPs can cross the blood-placental barriers and localized in trophoblast cells of the placenta on Day-10 and 19 of gestation.

Conclusion: This study shaded more light on the reproductive toxicity and teratogenicity of 10 nm and 25 nm AuNPs on early embryonic development and their adverse effects on the pregnant female rats.

Keywords: Gold nanospheres; Pregnant rats; Implantation rate; Histopathological changes; TEM; Skeletal deformities.

Introduction

The recent advances in nanotechnology have led to the development of novel technologies and products that can be used in many fields of research and industry [1]. Gold nanoparticles (AuNPs) are among the most commonly used nanoparticles (NPs). Gold nanoparticles are widely used due to their unique chemical and optical properties, low toxicity, good biocompatibility, and surface modification of control ability [2,3]. They are extensively used in industrial and biomedical purposes such as cosmetics, catalysis, electronics, biological sensors, drug delivery, cancer diagnosis and therapy [4-6]. However, the high risk

of exposure to AuNPs has raised huge issues related to their possible reproductive toxicity in humans.

Females are notably vulnerable to NPs toxicity, which may not only affect their reproductive potentials but also it may affect the fetal development and early embryonic stages. Fetal exposure during pregnancy to AuNPs is influenced by the stage of embryonic/placental maturation, nanoparticle size and surface composition [7]. In mammals, NPs can cross the placental barrier and accumulate in both embryonic and surrounding extra-embryonic tissues [8,9], leading to toxic effects on fetal development and placenta [10]. Intravenous (i.v.) injection

of titanium dioxide (TiO₂) in pregnant mice evoked structural changes, reduced fetal development with and produced various abnormalities [11]. Also, maternal oral dose of TiO₂ increased fetal deformities and their mortality [12]. When mouse blastocysts were treated with 50 μM silver nanoparticles (AgNPs) in vitro, they exhibited considerably lower implantation rate and exaggerated resorption of post-implantation embryos and decreased fetal weight [13]. Exposure of zebra fish embryos to copper oxide nanoparticles (CuO-NPs) produced developmental anomalies [14]. Also, chitosan nanoparticles (CSNPs) might have long-term adverse biological effects on pregnancy outcomes in mice [15]. On the other hand, AuNPs did not accumulate in rat fetuses and there is no evidence of fetal toxicity, despite it can cross the placenta into the fetus [16,17]. Taylor et al. [15] recorded that in mouse 2-cell stage embryos that were treated with 50 μg/ml AuNPs and cultured to the blastocyst stage, AuNPs did not show any detrimental effects on the development of mouse embryos.

Very few studies have been conducted on the direct effects of NPs on early stages of embryonic development. The direct exposure of early embryonic stages to AuNPs, and their subsequent effect on the fetal development, implantation rate has not been explored. Therefore, this study was designed to evaluate the effects of i.p. injection of AuNPs of different sizes (10 nm, 25 nm and 50 nm in diameter) during the early embryonic development on fetal development, implantation rate, fetal weight, histopathological changes, crossing blood-placental barrier and fetal skeletal deformities in pregnant rats.

Materials and methods

Chemicals

All chemicals used in the present work were purchased from Sigma-Aldrich Co. Germany unless otherwise mentioned. Ten nanometer gold nanoparticles (Cat. No. 7525984, Lot MK-BR9424V) were purchased from Sigma-Aldrich, Germany, with absorption 510-525 nm and concentration of 6.0 x 10¹² particles/ml.

Synthesis and characterization of gold nanospheres of 25 nm and 50 nm

Twenty-five and 50 nm gold nanoparticles were prepared by using citrate reduction method according to the method adopted by Turkevich [19] and Frens [20]. For the preparation of 25 nm and 50 nm GNPs, in two separate and clean conical flasks add 100 ml aqueous solution of 0.25 mM HAuCl₄ and heated to boiling with stirring. After that 1.5 ml or 3.5 ml of 1% aqueous solution (wt/v) of sodium citrate were added for 25 nm and 50 nm GNPs, respectively. Heating was maintained until a deep ruby red color was developed indicating the formation of gold nanoparticles. The boiling and stirring were extended for 30 min, and then cooled to room temperature.

Transmission electron microscopy and UV-Vis spectrometry measurements were used to characterize the prepared gold nanoparticles.

Animals and AuNPs exposure

Forty-eight mature female Albino rats (12 weeks old, 200±20 gm) were purchased from the Egyptian Holding Company for Biological Products and Vaccines (VACSERA, Egypt). Animals were housed individually in clean plastic cages with steel toppings with 12/12 hrs day and night cycle, the temperature was ranged between 20-25°C with a relative humidity of 55±5%. Food and

water were added ad libitum. After two weeks of adaptation, female rats were mated overnight (1:3 male to female), and Day-1 of pregnancy was defined as the day in which the mucous plug was detected and the presence of spermatozoa in vaginal smears.

On the second day of pregnancy, rats were randomly divided into four groups (12 pregnant rats per group) as follows: Control group: in which pregnant rats were injected with 1 ml normal saline solution i.p. on the 2nd day of gestation. For the 2nd, 3rd and 4th groups, pregnant rats were i.p. injected with 75 μg/kg body weight of 10 nm, 25 nm or 50 nm AuNPs, respectively.

In all groups, four animals were scarified, and the gravid uteri were dissected out on Days-10, 15 and 19 of pregnancy. Dissected uteri were checked for the distribution and resorption of fetus in the two uterine horns. On Day-19 of gestation, fetuses from control and experimental groups were recovered from the pregnant uteri and weighed.

Histological studies

On Day-10 and 19 of gestation, biopsy samples from pregnant uterus for control and experimental groups were fixed in 10% formalin solution for 48 h, then dehydrated in graded alcohol (50%, 70%, 80%, 90% and 100%), cleared in xylene and embedded in paraffin blocks. Sections (5 μm) were cut with rotary microtome, stained with hematoxylin–eosin, and observed under microscope (Olympus, Japan) according to the method adopted by Bancroft and Gamble [21]. All samples were examined by the same operator and photographs were captured with CCD camera Olympus DP12 attached to the microscope.

Electron microscopy

To study if AuNPs can cross blood-placental barrier, biopsy samples from placenta of control and 10 nm, 25 nm and 50 nm AuNPs injected groups were collected on Day-10 and 19 of pregnancy and fixed in 2.5 % glutaraldehyde, then fixed by immersion in 1% osmium tetra-oxide and washed in 0.1M sodium cacodylate buffer. Fixed and washed specimens were dehydrated through an ascending grade of alcohol, and then embedded in propylene oxide. Semi thin sections (1 μm thick) were cut using glass knives and stained with toluidine blue. Ultra-thin sections (50-80 nm thick) were cut using diamond knife and loaded on copper grids. The sections were double stained in uranyl acetate followed by lead citrate. Stained sections on grids were washed and examined by using JEOL 1010 Transmission Electron Microscope (TEM).

Skeletal malformation

On Day-19 of gestation, fetuses were fixed in 10% formalin for 7 days to dissolve the body fats, and then transferred to 2% potassium hydroxide (KOH) for three days to clear the skeletons, followed by applying Alizarin red stain dissolved in 2% KOH for two days to stain the ossified skeletal bones. After staining, clearing of the skeleton was carried out by passing the fetuses through the different concentration of glycerin and 2% KOH, and then fetuses were examined for skeletal anomalies. Finally, the fetuses were stored in pure glycerin in according to the methods of previously described by Globus and Gibson [22].

Statistical analysis

The statistical package for social sciences SPSS/PC computer program (version 20) was used for statistical analysis of the results. Data were analyzed using one-way analysis of variance

(ANOVA). The data were expressed as mean \pm S.E. Differences were considered statistically significant at ($P < 0.05$).

Results

Synthesis and characterization of gold nanospheres

Transmission Electron Microscope (TEM) images of 10 nm, 25 nm and 50 nm AuNPs were presented in Figure 1a-c. From these images, it is clear that, a uniform sphere shape of AuNPs with regular distribution were formed. The diameter of AuNPs was 10 nm, 25 nm and 50 nm for the small, medium and large size particle, respectively (Figure 1a,b,c). The surface Plasmon absorption of AuNPs was 525-530 nm.

Effect of AuNPs during early stage of pregnancy-on-pregnancy rate in female rats

Table 1 and Figures 2-4 represent the effects of i.p. injection of 75 $\mu\text{g}/\text{kg}$ body weight of 10 nm, 25 nm and 50 nm AuNPs on number of CL, fetus, and resorbed fetus on days 10, 15 and 19 of pregnancy in rats. The effects of exposure to different size AuNPs during the early embryonic development is size dependent. Results indicated that on day 10, 15 and 19 of pregnancy, the numbers of CL were similar in control and all the AuNPs injected pregnant rats (Table 1). Also, the number of fetuses was similar in control and all AuNPs injected rats on Day-10 of pregnancy. However, on day 15 and 19 of pregnancy, the number of fetuses was significantly ($P < 0.05$) lower, and the number of resorbed fetuses was higher ($P < 0.05$) in pregnant rats injected with 10 nm AuNPs when compared with control group. Meanwhile, on Day-19 of pregnancy, number of fetuses was lower ($P < 0.05$) and number of resorbed fetuses was higher ($P < 0.05$) in 25 nm AuNPs injected rats compared with control one.

Morphological assessment of uteri in control group revealed symmetrical distribution of fetuses in both uterine horns on Day-10 of pregnancy, and no fetal resorption or other abnormalities were detected (Figure 2a). However, fetuses were unequally distributed in uteri dissected on Day-10 of pregnancy from 50 nm AuNPs injected group and they were hemorrhagic (Figure 2b). The 25 nm AuNPs injected group were similar to the control group (Figure 2c). While, in 10 nm AuNPs injected group, the two uterine horns were equal in size, however, number of fetuses were lower in the left than the right uterine horn indicating early resorption of fetuses in one horn (Figure 2d).

Morphological examination of dissected uterine horns on Day-15 of gestation indicated that the control group showed symmetrical distribution of fetuses in uterine horns, no fetal absorption or hemorrhage (Figure 3a). While uteri dissected from 50 nm and 25 nm of AuNPs injected group showed unequal distribution of fetuses in both uterine horns when compared with the control group (Figure 3b,c). Also, 10 nm AuNPs group showed early resorbed fetuses, shortening of one uterine horn compared to the other one (Figure 3d,e).

Meanwhile, morphological examination of uteri obtained on Day-19 of gestation revealed symmetrical distribution of fetuses in the uterine horns in control, 25 nm and 50 nm AuNPs groups, with multiple fetuses in the two uterine horns (Figure 4a,b,c). While, for 10 nm AuNPs groups, the two uterine horns were unequal in size with reduction in implantation sites and presence of late resorbed fetus (LR, Figure 4d,e).

To investigate the tissue biodistribution of AuNPs, we examined the presence of 10 nm, 25 nm and 50 nm AuNPs in placental tissues on Day-10 and 19 of pregnancy by using TEM. TEM

micrographs illustrated the uptake of 10 nm AuNPs in trophoblast cells of the placenta. AuNPs of 10 nm size were detected in placental tissue on Day-10 and 19 of pregnancy, and it is more abundant on Day-10 than on Day-19 of gestation. Particles were mainly localized as membrane-bound vesicles (Figure 5a,b for Day-10 and 19 of pregnancy in rats, respectively). In contrast, 25 nm and 50 nm AuNPs were not detected in placental tissue either on Day-10 or 19 of gestation.

Histopathological changes in uterus and placenta of pregnant rats exposed to AuNPs

Histological examination of cross section of utero-placenta of control rats on Day-10 of pregnancy showed normal utero-placenta with an average uterine wall, average myometrium consists of smooth muscle and the decidual cells develop from the endometrial cells and form the basic structural matrix of the decidual, average maternal blood sinusoid lining with trophoblast cells and fetal blood vessel lining with endothelium (Figure 6a,b). On the other hand, for 10 nm AuNPs group, histopathological examination of cross section of utero-placenta showed edematous uterine wall, degenerated decidua with sever vacuolated cells, dilated congested blood sinusoids, small areas of hemorrhage, maternal blood sinusoid with degenerated trophoblastic lining, fetal blood vessel with few red blood cells and degenerated fetal tissue (Figure 6c,d). Meanwhile, pregnant animal injected with 25 nm AuNPs showed markedly edematous myometrium, decidua showed few vacuolated cells with dilated congested blood vessels, average maternal blood sinusoid and fetal blood vessel and normal fetal tissue (Figure 6e,f). Rats injected with 50 nm AuNPs showed ruptured uterine wall with marked edema and dilated congested blood vessels, degenerated decidua with numerous vacuolated cells and areas of hemorrhage (Figure 6g,h).

Moreover, on Day-19 of pregnancy, histopathological examination of utero-placenta in control rats illustrated normal structure, average myometrium and normal decidua and labyrinth zone and the basal zone. The basal zone is consisted of three types of differentiated cells: (1) spongiotrophoblasts, (2) trophoblastic giant cells and (3) glycogen cells, the spongiotrophoblasts were present immediately above the trophoblastic giant cell layer located at the materno-fetal placental interface. The glycogen cells form multiple small cell masses and develop into glycogen cell islands. In the labyrinth zone, there were three layers of trophoblasts, separating the maternal blood spaces from the fetal blood vessels. Also, blood vessels appeared in its normal structure. The outer trophoblast, which comes into direct contact with the maternal blood, is referred to as cytotrophoblasts and there were two layers of syncytiotrophoblasts (Figure 7a-d). While, the utero-placenta of 10 nm AuNPs injected rats showed marked edema of the myometrium and decidua, the trophospongium showed excess glycogen cells with apoptotic trophoblasts and labyrinth zone showing area of hemorrhage with narrow maternal sinusoids, fetal blood vessels containing few nucleated red cells and thin trophoblastic septa with giant trophoblasts and markedly dilated fetal blood vessels (Figure 7e-h). Similarly, pregnant rats injected with 25 nm AuNPs showed decidua with dilated congested blood vessel and trophospongium with few glycogen cells and congested blood vessels, apoptotic trophoblasts and vacuolation, while labyrinth zone with irregular maternal sinusoids; fetal blood vessels containing hemolyzed red blood cells and necrotic trophoblastic septa (Figure 7i-l). In 50 nm AuNPs injected pregnant animals illustrated decidua with an area of necrosis, the trophospongium

with congested blood vessels, few glycogen cells and cytolysis and apoptosis in trophoblastic giant cells. The labyrinth zone showed narrow maternal sinusoids, fetal blood vessels with few nucleated red blood cells and thin trophoblastic septa indicating the presence of apoptotic trophoblasts (Figure 7m-p).

Body weight of fetuses

The effect of i.p. injection of 10 nm, 25 nm and 50 nm AuNPs on foetal weight on Day-19 of gestation was illustrated in Figure 8. Data obtained indicated a significant difference in the foetal body weight between the control and AuNPs injected animals. Foetal body weight significantly ($P < 0.05$) decreased on Day 19 of gestation in 10 nm and 25 nm AuNPs injected rats when compared with control group (Figure 8). While foetal body weight on day-19 of gestation was non significantly lower 50 nm AuNPs group on Day-19 of gestation than the control one.

Ossification of the skull

On Day-19 of gestation, in the control group, the skeletal system was deeply stained with Alizarin red stain and showed complete ossification of all various parts of the skull, fore limb, thoracic and vertebral as well as the hind limb bones (Figure 9a-d). For 10 nm AuNPs group, retrieved fetuses on Day-19 of gestation showed incomplete ossification of the skull bones, absence of carpal and metacarpal bones of the fore limb, lacking most of the thoracic and vertebral and hind limb bones when compared with the corresponding control animals (Figure 9e-h). Fetuses retrieved in 25 nm AuNPs showed complete ossification of the different parts of the skeletal system except for the incomplete ossification of interparietal bone of the skull and lacking of the metacarpal bone of the fore limb (Figure 9i-l). In 50 nm AuNPs injected rats, ossification of the skull, fore and hind limbs, thoracic and vertebral bones were comparable to that in the control group (Figure 9m-p).

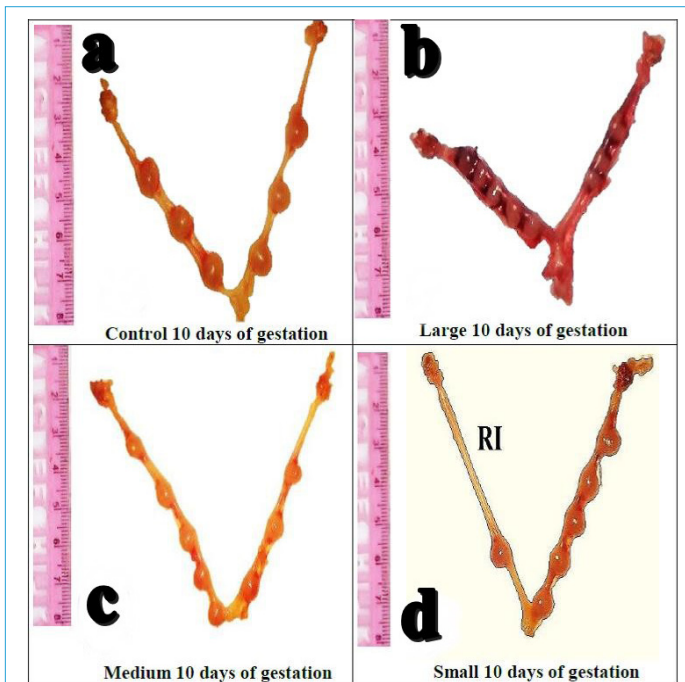
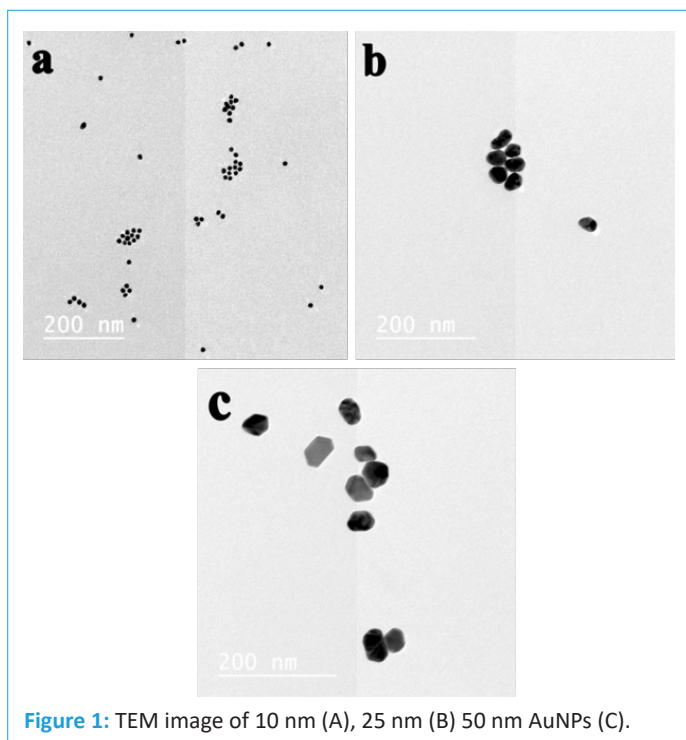


Figure 2: Photograph for pregnant uteri obtained from control and AuNPs injected female pregnant rats on Day-10 of gestation. Control group (a), 50 nm AuNPs group (b), 25 nm AuNPs group (c), and 10 nm AuNPs group (d).

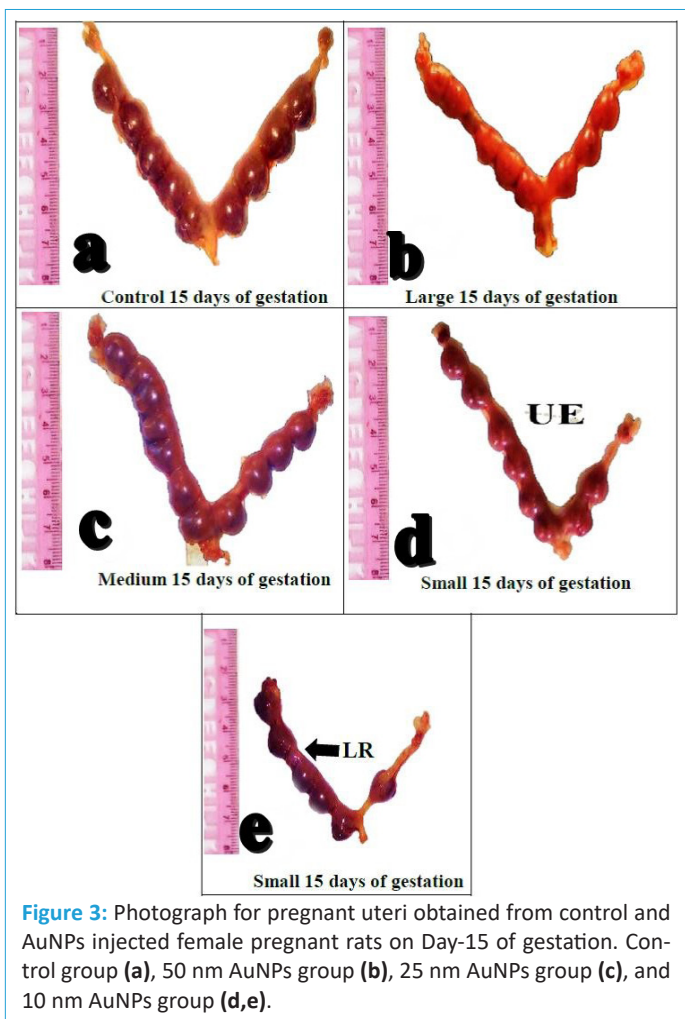


Figure 3: Photograph for pregnant uteri obtained from control and AuNPs injected female pregnant rats on Day-15 of gestation. Control group (a), 50 nm AuNPs group (b), 25 nm AuNPs group (c), and 10 nm AuNPs group (d,e).

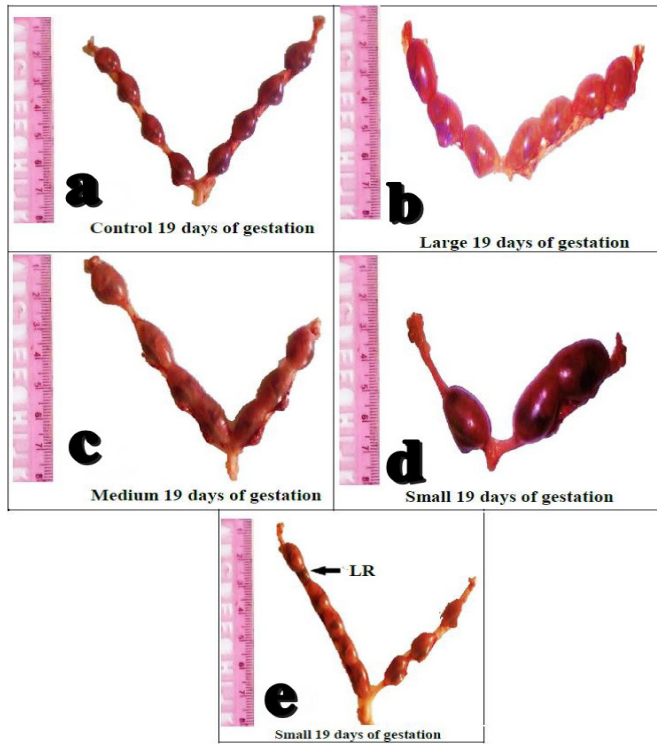


Figure 4: Photograph for pregnant uteri obtained from control and AuNPs injected female pregnant rats on Day-19 of gestation. Control group (a), 50 nm AuNPs group (b), 25 nm AuNPs group (c) and 10 nm AuNPs group (d,e).

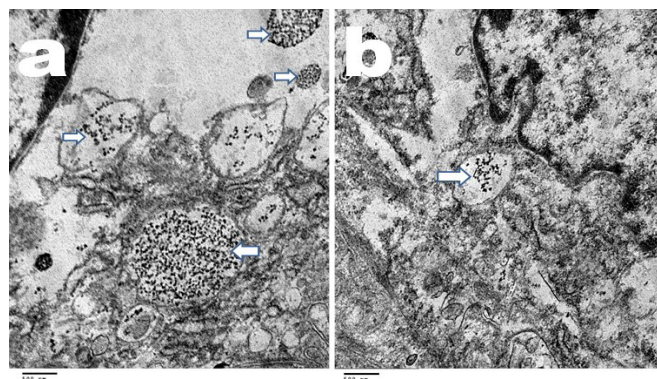


Figure 5: Photomicrograph for localization of 10nm AuNPs in trophoblast cells of the placenta (white arrows) on Day-10 (A) and Day-19 of gestation (B).

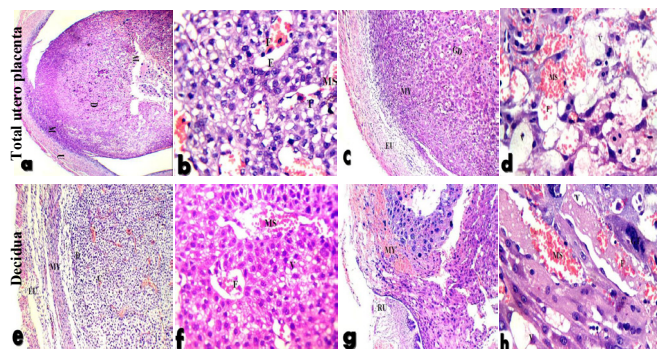


Figure 6: Photomicrograph of uterine sections in control group (A,B), 10 nm AuNPs injected animals (C,D), 25 nm AuNPs (E,F), and pregnant rats injected with 50 nm AuNPs (G,H) (H&E X100, 400).

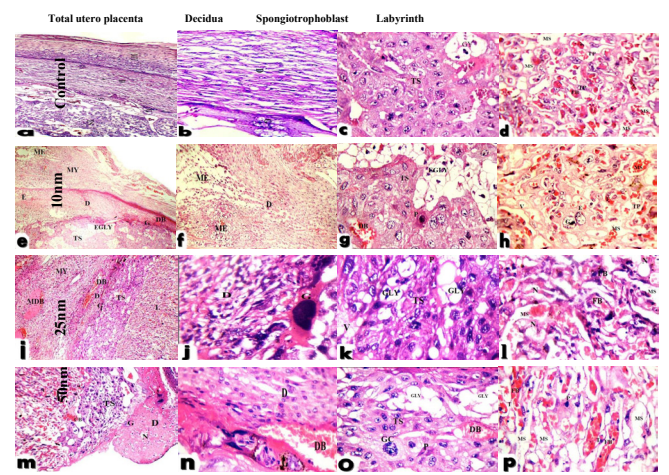


Figure 7: Photomicrograph of placenta sections in control group showing utero-placenta, decidua, spongiotrophoblast and labyrinth zone on Day-19 of gestation in control (a-d), 10 nm AuNPs injected (e-h), 25 nm AuNPs group (i-l), and 50 nm AuNPs (m-p) (H&E X100, 400).

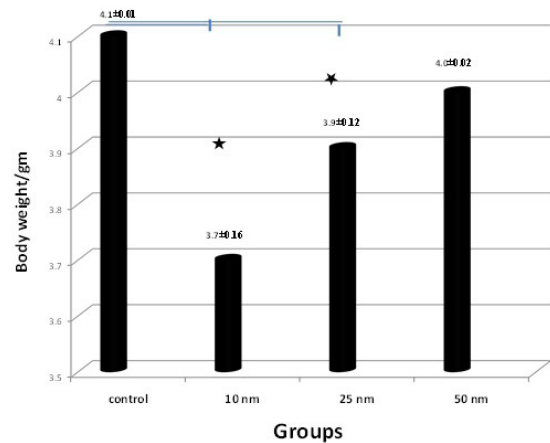


Figure 8: The effect of injection of AuNPs of different size on fetal body weight/gm on Day-19 of gestation.

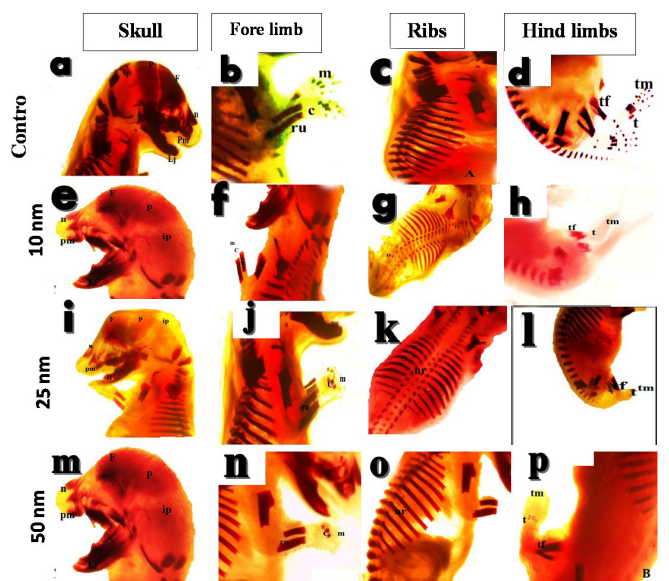


Figure 9: Photograph showing skull bones, fore limb, thoracic and vertebral bones and hind limb for fetuses retrieved on Day-19 of pregnancy and stained with Alizarin red in control (a-D), 10 nm AuNPs injected rats (e-h), 25 nm injected pregnant rats (i-l), and 50 nm AuNPs group (m-p).

Table 1: Effect of i.p. injection of 10 nm, 25 nm and 50 nm AuNPs at the early stage of embryonic development on number of CL, fetuses and resorbed fetuses on Day 10, 15 and 19 of pregnancy in rats (Mean±SEM).

Item	Days of pregnancy																	
	Day-10						Day-15						Day-19					
	10 nm		25 nm		50 nm		10 nm		25 nm		50 nm		10 nm		25 nm		50 nm	
	Con	Au	Con	Au	Con	Au	Con	Au	Con	Au	Con	Au	Con	Au	Con	Au	Con	Au
No. CL	8.0±0.5	6.8±0.7	8.0±0.5	7.6±0.2	8.0±0.5	7.6±0.4	7.2±0.6	8.0±0.3	7.2±0.6	8.8±0.6	7.2±0.6	7.6±0.5	7.0±0.5	8.0±0.5	7.0±0.5	7.0±0.5	7.0±0.5	8.0±0.6
No. Fetus	8.0±0.5	6.8±0.7	8.0±0.5	7.0±0.3	8.0±0.5	7.0±0.5	7.2±0.6	6.2±0.4 [*]	7.2±0.6	7.8±0.8	7.2±0.6	7.6±0.5	7.0±0.5	5.6±0.7 [*]	7.0±0.5	5.8±0.7 [*]	7.0±0.5	7.8±0.6
Resorbed	0.0±0.0	0.0±0.0	0.0±0.0	0.0±0.0	0.0±0.0	0.0±0.0	0.0±0.0	0.6±0.2 [*]	0.0±0.0	0.0±0.0	0.0±0.0	0.2±0.2	0.0±0.0	0.6±0.2 [*]	0.0±0.0	0.6±0.2 [*]	0.0±0.0	0.2±0.2

Con: Control; Au: AuNPs; *Superscript within the same row differ significantly at P<0.05.

Discussion

With the widespread use of AuNPs in various industrial and scientific fields, major human safety concerns are developed especially among the pregnant women. During pregnancy, exposure to nanoparticles has adverse effects on fetal development and placenta, therefore, assessment of embryo-fetal toxicity is a prerequisite for the use of gold nanoparticles during gestation [11].

The data presented in this study showed for the first time the transplacental size and time-dependent effects of AuNPs on maternal-embryo-fetal development in rats, thus highlighting new aspects related to the putative reproductive toxicity and teratogenic effects of AuNPs during this vulnerable lifespan. On Day-10 of gestation, which coincides with maturation of the placental rat's blood supply and placenta barrier function, the present work revealed that number of CL, fetuses and resorbed fetuses did not vary between control and the experimental groups. However, on Day-15 gestation in rats, the number of fetuses was lower (P<0.05) and the number of resorbed fetuses was significantly higher (P<0.05) in 10 nm AuNPs injected pregnant rats when compared with control or 25 nm or 50 nm AuNPs injected group. The same findings were also observed for the 10 nm injected rats on Day-19 of gestation. In addition, the number of resorbed fetuses was higher (P<0.05) in the 25 nm AuNPs injected group than in 50 nm AuNPs or control groups on Day19 of gestation. These findings were accompanied by a significantly lower fetal weight (P<0.05) in 10 nm and 25 nm AuNPs injected groups compared to control or 50 nm injected group. In addition, morphological assessment of uterine horns on Day-10 of pregnancy revealed that the two uterine horns were unequal in size and that the fetuses were unequally distributed between the two uterine horns in the 10 nm AuNPs group compared to control or the other AuNPs size. While, on Day-15 of pregnancy, the two uterine horns were asymmetrical in size in 25 nm and 50 nm injected rats when compared with control. While, in 10 nm AuNPs injected rats shortening of one of the uterine horns was detected due to the higher number of resorbed fetuses. On Day-19 of pregnancy, injection of 10 nm or 25 nm AuNPs leads to asymmetrical size of the two uterine horns with higher incidence of fetal resorption when compared with control or 50 nm injected group. According to our knowledge this is the first study to compare the effect of AuNPs of different size on fetal development in rats. Similarly, exposure of mouse blastocysts to AgNP in vitro can induce apoptosis in the trophectoderm and the inner cell mass with significant inhibition cell proliferation, the implantation ratio was significantly lower and the potential of embryos for subsequent development was failed when compared to the untreated controls [8]. Also, TiO₂ induced a

smaller size of uteri and fetuses [12], increased fetal deformities and mortality in pregnant mice [13]. In addition, quantum dots (QD) inhibited cell proliferation; primarily in the inner cell mass, inhibited post-implantation embryonic development, and were associated with absorption of post-implantation blastocysts and a decrease in fetal weight [23]. In contrast, single injection of gold nanorods (AuNRs) did not impaired reproductive potentials in cats [24]. Meanwhile, repeated exposure of pregnant rats to zinc oxide nanoparticles (ZnONPs) has no effect of the number of corpora lutea, number of implantation sites, the implantation rate, dead fetuses [25]. Also, there were no signs of developmental abnormalities or stress was detected in AuNPs treated pregnant mice. All the pups in the AuNPs treated groups delivered at term and fetal counts were comparable with controls [26]. This discrepancy may be due to species difference, particles shape, dose, size or the route of administration, or the stage of pregnancy at which AuNPs were injected.

Moreover, in the current work, i.p. 10 nm or 25 nm AuNP injection during early embryonic development resulted in a significant reduction (P<0.05) in fetal weight compared to the control or 50 nm group. In contrast, there were no reductions in fetal weight in AuNPs treated pregnant rats compared to control one [27]. This difference may be due to the nanoparticle size or the stage of pregnancy at which AuNPs were injected or the route of administration.

Furthermore, the present work demonstrated the ability of 10nm AuNPs to cross blood-placental barriers and internalize into pregnant rats placenta. Ten nanometer AuNPs can cross the blood-placental barriers and were detected in lysosomes and membrane bound vesicles in cytoplasm of the trophoblast cells of the placenta, and it is more abundant on Day-10 than Day-19 of pregnancy. While 25 nm and 50 nm AuNPs were not detected in placenta either on day-10 or 19 of pregnancy. Similar results were previously reported using other NPs [9,27]. These findings are consistent with that reported by Semmler-Behnke et al. [17] who found that the localization of AuNPs in placenta and fetus is size dependent in Wistar rats. NP penetrated through the placenta by active transcellular transport or directly by injured the placental barriers [12]. In contrast, after i.v. or i.p. injection of 2 and 40 nm AuNPs in pregnant C57BL/6 mice, no transfer was observed 1, 4, and 24 h after injection [28]. These findings inconsistencies may be due to sampling time, various AuNP preparation protocols, size or dose used.

To understand the mechanism of reproductive toxicity of AuNPs in pregnant rats, histopathological examination of rat placenta is essential in the safety assessment of nanoparticles [29]. In this work, i.p. injection of 10 nm, 25 nm or 50 nm AuNPs on Day-2 of gestation produced histopathological changes in

the uterus and placenta in pregnant rats. In rats scarified on Day-10 of gestation, 10 nm and 25 nm AuNPs produced degenerative changes in decidua in the form of vacuolated cells with dilated congested blood vessels. In animals treated with 50 nm, ruptured uterine wall with protrusion of trophoblastic tissue outside the uterine cavity and areas of hemorrhage were recorded. Moreover, for animals scarified on Day-19 of pregnancy, the present study demonstrated that animals injected with 10 nm or 50 nm AuNPs showed decidua with marked edema and area of necrosis. Also, trophospongium zone with few glycogen cells and congested blood vessels were recorded in the animals treated with 25, 50 nm AuNPs. While, in animals treated with 10 nm AuNPs, the labyrinth area showed degenerated trophoblastic septa, hypoplasia and increasing in incidence of apoptotic cells. According to our knowledge this is the first study to evaluate the utero-placental histopathological changes at different stages of gestation after exposure to different sizes of AuNPs in rats. In concomitant, when zebra fish embryos were exposed to SiO₂ nanoparticles, the nanoparticles adhered to the surface of the chorion and caused damage in decidual layer [30]. Zhang et al. [31] showed that the area of placental spongiotrophoblast significantly increased and labyrinth was markedly reduced in mice treated with TiO₂ NP when compared with control group. Maternal exposure to chemicals may induce placental injuries and subsequently lead to placental dystrophy, reproductive toxicity, impaired fetal growth and development as well as congenital malformations [32,33]. On the other hand, there is no evidence of accumulation of AuNPs in rat fetuses or signs of fetal toxicity can occur across the uterus into the placenta [16,17]. This discrepancy may be associated with AuNPs injection time, dose or size of the gold nanoparticles used.

In addition, during the first 48 h of embryo development, the exposure of rat embryos to AuNPs produced skeletal deformities in fetuses recovered on gestation Day-19. In pregnant rats injected with 10 nm AuNPs, this effect was more severe. This group showed skeletal deformity nearly in all the skeletal bones including head, fore and hind limbs, ribs, and cervical and thoracic bones. This deformity ranged from incomplete bone ossification to the complete absence of some bones, especially in the fore and hind limbs and vertebral column. Also, 25 nm and could produce some incomplete ossification of interparietal bone in the skull and lacking metacarpal bone in the fore limb. At the same time, 50 nm AuNPs has no adverse effect on skeletal development in pregnant rats. According to our knowledge this is the first study on the possible teratogenic effect of AuNPs on rat fetuses. Similarly, Single Walled Carbon Nanoparticles (SW-CNTs) appeared to be embryo lethal, teratogenic, and induced death and growth retardation when administered to pregnant mice [34], or chicken embryo [35]. An oral administration of TiO₂ NPs in a high single dose of 100 or 1,000 mg/kg to pregnant dams causes a significant increase in fetal deformities and mortality [36]. In other studies, pup mortality increased during the lactation period and decreased growth without deformities was detected at concentrations of 0.25, 0.5, and 1 mg platinum (Pt) NPs/kg when given 14 days before and 4 days after mating in mice [37]. Also, injection of quantum dots (QD) on Day-13 of pregnancy in mice resulted in a reduction in fetal body weight and disturbed ossification of limbs and placental tissue damage [38]. On contrary, when Wistar rats were injected with QDs, QD did not cause any embryo-toxic or teratogenic effects, and microscopic tissue testing revealed that QDs accumulated in the placenta but did not penetrate the embryonic tissue [39]. Also, AgNPs did not cause any developmental toxicity to pregnant

rats [40]. This discrepancy may be due to the difference in the type of particles, or the animal model used for research or the stage at which NPs were administered.

Conclusion

10 nm AuNPs are embryo toxic when administered in rats during the early stage of embryo development as indicated by retarding embryo growth, increased incidence of fetal resorption and teratogenicity. The mechanism by which AuNPs could produce teratogenic effect was not previously investigated, so it is compulsory to expand our knowledge to the role of 10 nm and 25 nm AuNPs in teratogenicity to exclude the safety risks associated with their potential biomedical use.

Declarations

Ethical approval: All the procedures performed in the current study were in accordance with the Guide for the Care and Use of Laboratory Animals published by the US National Institutes of Health (NIH Publication No. 85-23, revised 1996) and was approved by Committee for Animal Care, National Research Centre of Egypt, and the Ethical Committee for Faculty of Science Al-Azhar University, Egypt.

Acknowledgement: Authors are gratefully acknowledging the financial support provide by Misr El-Kheir Foundation to conduct this work (Proj. ID: LGA03150032, Applications of photothermal therapy using gold nanoparticles in cancer).

Author's contribution: ASSA designed the work, ASSA and OFA conduct the experimental work, ASSA and OFA did, ASSA drafted the manuscript. All authors were involved in scientific discussion, analysis of the data and revising the manuscript.

Availability of data: The dataset obtained and analyzed from this work were presented at the text and the original data will be available upon request.

Competing interests: The authors declare that they have no competing interests.

References

1. Hassan AA, Abdoon ASS, Elsheikh SM, Khairy MH, Gamal Eldin AA, et al. Effect of acute gold nanorods on reproductive function in male albino rats: histological, morphometric, hormonal, and redox balance parameters. *Environ Sci Pollut Res.* 2019; 26: 15816-15827.
2. Kang B, Mackey MA, El-Sayed MA. Nuclear targeting of gold nanoparticles in cancer cells induces DNA damage, causing cytokinesis arrest and apoptosis. *J Am Chem Soc.* 2010; 132: 1517-1519.
3. Kang B, Austin LA, El-Sayed MA. Real-time molecular imaging throughout the entire cell cycle by targeted plasmonic-enhanced Rayleigh/Raman spectroscopy. *Nano Lett.* 2012; 12: 5369-5375.
4. Jeong EH, Jung G, Hong CA, Lee H. Gold nanoparticle (AuNP)-based drug delivery and molecular imaging for biomedical applications. *Arch Pharm Res.* 2014; 37: 53-9.
5. Liu H, Wang J, Feng Z, Lin Y, Zhang L, Su D. Facile synthesis of Au nanoparticles embedded in an ultrathin hollow graphene nanoshell with robust catalytic performance. *Small.* 2015; 11: 5059-5064.
6. Abdoon AS, Al-Ashkar EA, Kandil OM, Shaban AH, Khaled HM, et al. Efficacy and toxicity of plasmonic photothermal therapy (PPTT) using gold nanorods (GNRs) against mammary tumors in

- dogs and cats. *Nanomedicine*. 2016; 12: 2291-2297.
7. Cho WS, Cho M, Jeong J, Choi M, Han BS, et al. Size-dependent tissue kinetics of PEG-coated gold nanoparticles. *Toxicol Appl Pharmacol*. 2010; 245: 116-23.
 8. Li PW, Kuo TH, Chang JH, Yeh JM, Chan WH. Induction of cytotoxicity and apoptosis in mouse blastocysts by silver nanoparticles. *Toxicol. Lett*. 2010; 197: 82-7.
 9. Chu M, Wu Q, Yang H, Yuan R, Hou S, Yang Y, et al. Transfer of quantum dots from pregnant mice to pups across the placental barrier. *Small*. 2010; 6: 670-678.
 10. Huang JP, Hsieh PC, Chen CY, Wang TY, Chen PC, et al. Nanoparticles can cross mouse placenta and induce trophoblast apoptosis. *Placenta*. 2015; 36: 1433-31.
 11. Muller EK, Grafe C, Wiekhorst F, Bergemann C. Magnetic nanoparticles interact and pass an in vitro co-culture blood-placenta barrier model. *Nanomaterials*. 2018; 8: pii: E108.
 12. Yamashita K, Yoshioka Y, Higashisaka K, Mimura K, Morishita Y, et al. Silica and titanium dioxide nanoparticles cause pregnancy complications in mice. *Nat. Nanotech*. 2011; 6: 321-8.
 13. Philbrook NA, Winn LM, Afroz AR, Saleh NB, Walker VK. The effect of TiO₂ and Ag nanoparticles on reproduction and development of *Drosophila melanogaster* and CD-1 mice. *Toxicol Appl Pharmacol*. 2011; 257: 429-36.
 14. Ganesan S, Thirumurthi NA, Raghunath A, Vijayakumar S, Perumal E. Acute and sub-lethal exposure to copper oxide nanoparticles causes oxidative stress and teratogenicity in zebrafish embryos. *J Appl Toxicol*. 2016; 36: 554-67.
 15. Park MR, Gurunathan S, Choi, YJ, Kwon DN, Han JW, Cho SG, et al. Chitosan nanoparticles cause pre-and postimplantation embryo complications in mice. *Biol Reprod*. 2013; 88: 88.
 16. Rattanpinyopituk K, Shimada A, Morita T, Sakurai M, Asano A, Hasegawa T, et al. Demonstration of the clathrin-and caveolin-mediated endocytosis at the maternal-fetal barrier in mouse placenta after intravenous administration of gold nanoparticles. *J Vet Med Sci*. 2014; 76: 377-387.
 17. Semmler-Behnke M, Lipka J, Wenk A, Hirn S, Schäffler M, et al. Size dependent translocation and fetal accumulation of gold nanoparticles from maternal blood in the rat. *Part Fibre Toxicol*. 2014; 11: 33.
 18. Taylor U, Garrels W, Barchanski A, Peterson S, Sajti L, et al. Rath, Injection of ligand-free gold and silver nanoparticles into murine embryos does not impact pre-implantation development. *Beilstein J Nanotechnol*. 2014; 5: 677-688.
 19. Turkevitch T, Stevenson PC, Hillier J. A study of the nucleation and growth processes in the synthesis of colloidal gold. *Discuss Faraday Soc*. 1951; 11: 55-75.
 20. Frens G. Controlled nucleation for the regulation of the particle size in monodisperses gold suspensions. *Nat Phys Sci*. 1973; 241: 20-22.
 21. Bancroft JD, Gamble M. Theory and practice of histological techniques. 5th ed. Edinburgh. New York, London, Philadelphia Churchill Livingstone pub. 2002; 125-138.
 22. Globus M, Gibson MA. A histological study of the development of the sternum in thalidomide treated rats. *Teratology*. 1968; 1: 235-256.
 23. Chan, WH, Shiao NH. Cytotoxic effect of CdSe quantum dots on mouse embryonic development. *Acta Pharmacol Sin*. 2008; 29: 259-66.
 24. Abdoon AS, Al-Ashkar EA, Shabaka A, Kandil OM, Eisa WH, et al. Normal pregnancy and lactation in a cat after treatment of mammary gland tumor when using photothermal therapy with gold nanorods: A case report. *Journal of Nanomedicine and Nanotechnology*. 2015; 6: 1.
 25. Hong JS, Park MK, Kim MS, Lim JH, Park GJ, et al. Effect of zinc oxide nanoparticles on dams and embryo-fetal development in rats. *Int J Nanomedicine*. 2014; 15: 145-57.
 26. Yang H, Sun C, Fan Z, Tian X, Yan, et al. Effects of gestational age and surface modification on materno-fetal transfer of nanoparticles in murine pregnancy. *Sci Rep*. 2012; 2: 847.
 27. Yang H, Du L, Tian X, Fan Z, Sun C, et al. Effects of nanoparticle size and gestational age on maternal biodistribution and toxicity of gold nanoparticles in pregnant mice. *Toxicol Lett*. 2014; 230: 10-8.
 28. Sadauskas E, Wallin H, Stoltenberg M, Vogel U, Doering P, et al. Kupffer cells are central in the removal of nanoparticles from the organism. *Part Fibre Toxicol*. 2007; 4: 10.
 29. Furukawa S, Hayashi S, Usuda U. Toxicological pathology in the rat placenta. *J Toxicol Pathol*. 2011; 24: 95-111.
 30. Fent K, Weisbrod CJ, Wirth-Heller A, Pieleus U. Assessment of uptake and toxicity of fluorescent silica nanoparticles in zebrafish (*Danio rerio*) early life stages. *Aquat Toxicol*. 2010; 100: 218-228.
 31. Zhang L, Xi X, Zhou Y, Deng Y, Ouyang B, et al. Gestational exposure to titanium dioxide nanoparticles impairs the placentation through dysregulation of vascularization, proliferation and apoptosis in mice. *Inter. J Nanomed*. 2018; 13: 777-789.
 32. Syme MR, Paxton JW, Keelan JA. Drug transfer and metabolism by the human placenta. *Clin Pharmacokinet*. 2004; 3: 487-514.
 33. Wick P, Malek A, Manser P, Meili D, Maeder-Althaus X, et al. Barrier capacity of human placenta for nanosized materials. *Environ. Health Perspect*. 2010; 118: 432-436.
 34. Ema M, Gamo M, Honda K. Developmental toxicity of engineered nanomaterials in rodents. *Toxicol Appl Pharmacol*. 2016; 15: 47-52.
 35. Ema M, Hougaard KS, Kishimoto A, Honda K. Reproductive and developmental toxicity of carbon-based nanomaterials: A literature review. *Nanotoxicology*. 2016; 10: 391-412.
 36. Park E, Bae, E. Repeated-dose toxicity and inflammatory responses in mice by oral administration of silver nanoparticles. *Environ. Toxicol. Pharm*. 2010; 30: 162-168.
 37. Pietroiusti A, Massimiani M, Fenoglio I, Colonna M, Valentini F, et al. Low doses of pristine and oxidized single-wall carbon nanotubes affect mammalian embryonic development. *ACS Nano*. 2011; 5: 4624-33.
 38. Zalgevičienė V, Kulvietis V, Bulotienė D, Didžiapetrienė J, Rotomskis R. The effect of nanoparticles in rats during critical periods of pregnancy. *Medicina (Kaunas)*. 2012; 48: 256-64.
 39. Zalgevičienė V, Kulvietis V, Bulotienė D, Zurauskas E, Laurinavičienė A, et al. Quantum dots mediated embryotoxicity via placental damage. *Reprod Toxicol*. 2017; 73: 222-231.
 40. Yu WJ, Son JM, Lee J, Kim SH, Lee IC, et al. Effects of silver nanoparticles on pregnant dams and embryo-fetal development in rats. *Nanotoxicology*. 2014; 185-91.